Deuterium Off-Resonance Rotating Frame Spin-Lattice Relaxation of Macromolecular Bound Ligands

Jan M. Rydzewski and Thomas Schleich
Department of Chemistry and Biochemistry, Sinsheimer Laboratories, University of California, Santa Cruz, California 95064 USA

ABSTRACT Deuterated 3-trimethylsilylpropionic acid binding to bovine serum albumin was used as a model system to examine the feasibility and limitations of using the deuterium off-resonance rotating frame spin-lattice relaxation experiment for the study of equilibrium ligand-binding behavior to proteins. The results of this study demonstrate that the rotational-diffusion behavior of the bound species can be monitored directly, i. e., the observed correlation time of the ligand in the presence of a protein is approximately equal to the correlation time of the ligand in the bound state, provided that the fraction of bound ligand is at least 0.20. The presence of local ligand motion and/or chemical exchange contributions to relaxation in the bound state was inferred from the observation that the correlation time of the bound ligand was somewhat smaller than the correlation time characterizing the overall tumbling of the protein. An approximate value for the fraction of bound ligand was obtained from off-resonance relaxation experiments when supplemental spin-lattice or transverse relaxation times were employed in the analysis. Incorporation of local motion effects for the bound species into the theoretical relaxation formalism enabled the evaluation of an order parameter and an effective correlation time, which in conjunction with a wobbling in a cone model, provided additional information about ligand motion in the bound state.

INTRODUCTION

The off-resonance rotating frame spin-lattice relaxation experiment applied to spin 1/2 nuclei yields a rotational correlation time reflecting overall molecular reorientational motional behavior (Schleich et al., 1989, 1992). This magnetic resonance technique was recently shown to be applicable to the study of intermediate time scale molecular motions (correlation time range ca. 2–500 ns) of deuterium-labeled molecules (Rydzewski and Schleich, 1994), and is therefore an appropriate methodology for rotational-diffusion studies involving both in vitro as well as in vivo systems. This study extends the off-resonance rotating frame spin-lattice relaxation experiment to the investigation of the rotational diffusion behavior of deuterium-labeled ligands engaged in equilibrium binding to macromolecules.

Deuterated 3-trimethylsilylpropionic acid (TSP-d_4) binding to bovine serum albumin (BSA) was used as a model system to examine the feasibility and limitations of using the deuterium off-resonance rotating frame spin-lattice relaxation experiment for the study of equilibrium ligand-binding behavior to proteins. Several different motional models were incorporated in the off-resonance rotating frame spin-lattice relaxation formalism. Isotropic reorientational motion of the ligand in the free and bound states, both with and without the inclusion of fast exchange, was assumed. In addition, to more adequately account for the motional behavior of the deuterated ligand in the macromolecular bound state, the model-free approach of Lipari and Szabo (1982a, b) was included in the formalism. This method utilizes an order parameter and effective correlation time, in addition to an overall correlation time, to describe molecular motion, which in the case of fast internal motions provides unique dynamical information in the absence of a specific model. The derived formalism was used to illustrate the theoretical dependence of the spectral intensity ratio (R), a key characteristic of the off-resonance rotating frame spin-lattice relaxation experiment, on the relevant off-resonance irradiation and ligand-binding parameters. The formalism was also employed for the analysis of experimental binding data.

THEORY

The theoretical formalism describing the ^{2}H off-resonance rotating frame spin-lattice relaxation experiment has been presented in detail elsewhere (Rydzewski and Schleich, 1994; Schleich et al., 1989, 1992). The experiment involves the application of a continuous wave low power radio frequency (RF) irradiation field at a frequency off-resonance from the resonance(s) of interest for a time approximately equal to $5T_1$. The resulting reduction in signal intensity is assessed, and the spectral intensity ratio ($R = M_z/M_o$) is equal to $\cos^2\Theta\ [T_{1\rho}^{off}/T_1]$ where Θ is the angle between the effective field and the z-axis, and $T_{1\rho}^{off}$ and T_1 are the spin-lattice magnetic relaxation times of the nuclear spins in the presence and absence of the RF field, respectively. The angle Θ is dependent upon both B_2 and the frequency offset (ν_{off}) of the RF irradiation field. The theoretical expression for $1/T_{1\rho}^{off}$, the relaxation rate constant

Received for publication 23 June 1995 and in final form 16 November 1995.

Address reprint requests to Dr. Thomas Schleich, Department of Chemistry and Biochemistry, University of California, Santa Cruz, CA 95064. Tel.: 408-459-2067; Fax: 408-459-2935; E-mail: yoti@aku.ucsc.edu.

The present address of Dr. Rydzewski is: Department of Molecular Biology, The Scripps Research Institute, 10666 North Torrey Pines Road, La Jolla, CA 92037.

0006-3495/96/03/1472/13 $2.00

that describes spin relaxation along the effective field assuming axial symmetry for the electric field tensor, is (Rydzewski and Schleich, 1994):

$$\begin{aligned}\frac{1}{T_{1\rho}^{\text{off}}} = L\Bigg\{&\frac{3}{2}[\sin^2\Theta\cos^2\Theta J(\omega_e) + \sin^4\Theta J(2\omega_e)] \\ &+ \left[\cos^2\left(\frac{3\Theta}{2}\right)\cos^2\left(\frac{\Theta}{2}\right)J(\omega_o + \omega_e)\right. \\ &+ \sin^2\left(\frac{3\Theta}{2}\right)\sin^2\left(\frac{\Theta}{2}\right)J(\omega_o - \omega_e) \\ &+ \sin^2\Theta\cos^4\left(\frac{\Theta}{2}\right)J(2\omega_o + \omega_e) \\ &\left.+ \sin^2\Theta\sin^4\left(\frac{\Theta}{2}\right)J(2\omega_o - \omega_e)\right] \\ &+ 4\left[\sin^2\Theta\cos^4\left(\frac{\Theta}{2}\right)J(\omega_o + 2\omega_e)\right. \\ &+ \sin^2\Theta\sin^4\left(\frac{\Theta}{2}\right)J(\omega_o - 2\omega_e) \\ &+ \cos^8\left(\frac{\Theta}{2}\right)J(2\omega_o + 2\omega_e) \\ &\left.+ \sin^8\left(\frac{\Theta}{2}\right)J(2\omega_o - 2\omega_e)\right]\Bigg\}\end{aligned} \tag{1}$$

where

$$L = \frac{3}{80}\left[\frac{2\pi e^2 qQ}{h}\right]^2 \tag{2}$$

and ω_o is the Larmor precessional frequency of the nuclear spins, ω_e is the angular precessional frequency about the effective field, $(2\pi e^2qQ/h)$ is the quadrupolar coupling constant in rad/s, and $J(\omega)$ is the spectral density function, which is defined below. When ω_e and Θ are zero, Eq. 1 reduces to the familiar longitudinal relaxation rate constant expression for a spin 1 nucleus assuming axial symmetry of the electric field gradient. In liquids, where the rotational correlation time is much smaller than the magnitude of the quadrupolar interaction (i.e., $\tau_o \ll [h/e^2qQ]$), complete averaging of the quadrupolar interaction occurs, and thus quadrupolar splitting of the spectral lines can be ignored. Theoretical expressions for ^{2}H T_1 and T_2 relaxation times, assuming a dominant quadrupolar relaxation mechanism, are given elsewhere (Rydzewski and Schleich, 1994).

Isotropic reorientation

Assuming isotropic tumbling, the spectral density function appropriate for spin 1 quadrupolar relaxation is:

$$J(\omega) = \frac{2\tau_o}{1 + \omega^2\tau_o^2} \tag{3}$$

where τ_o is the correlation time for isotropic reorientational motion of a rigid spherical particle (Rydzewski and Schleich, 1994).

Chemical exchange

To accommodate equilibrium macromolecular deuterium-labeled ligand-binding considerations into the formalism of the off-resonance rotating frame spin-lattice relaxation experiment, the dependence of the spectral intensity ratio on molecular motion was modified. Fast exchange on the NMR relaxation time and chemical shift scales was assumed, and thus the $1/T_1$ and $1/T_{1\rho}^{\text{off}}$ relaxation rate constants used in the expression for the spectral intensity ratio were the sum of the relaxation rate constants of the free and the bound species weighted by their respective mole fractions. Similar considerations were assumed to apply to $1/T_2$, the transverse relaxation rate. Furthermore, the overall correlation time of the bound state, $\tau_{o,B}$, which represents binding of the ligand to macromolecular species, may include contributions from the lifetime of the bound nuclear spin (τ_{ex}), if τ_{ex} is approximately equal to or less than τ_o, the correlation time characterizing isotropic rotational motion, and is defined by the following expression:

$$\frac{1}{\tau_{o,B}} = \frac{1}{\tau_{rot}} + \frac{1}{\tau_{ex}} \tag{4}$$

(Marshall, 1970; Rose and Bryant, 1978).

Bound ligand internal motion

For a molecule, such as a bound ligand, experiencing internal motion superimposed on overall reorientational motion, the spectral density functions can be described using the model-free approach proposed by Lipari and Szabo (1982a, b). This approach is applicable to the case of an electric field gradient μ, reorienting by internal motion within a macromolecular framework, superimposed on overall isotropic reorientational motion described by a correlation time, τ_M. In the case of ligand binding, the deuterated molecule was assumed to have a fixed point of attachment, whereas μ was allowed restrained freedom of motion within the binding site. The spectral density function is:

$$J(\omega) = 2\left[\frac{S^2\tau_M}{1 + \omega^2\tau_M^2} + \frac{(1 - S^2)\tau}{1 + \omega^2\tau^2}\right] \tag{5}$$

where $\tau^{-1} = \tau_M^{-1} + \tau_e^{-1}$; S^2 is the generalized order parameter ($0 \le S^2 \le 1$) that reflects the degree of spatial restriction of motion of the deuterium nucleus of the bound metabolite and is model independent, and τ_e is the effective correlation time reflecting the temporal scale of the internal motion. For a rigidly attached deuterated ligand ($S^2 = 1$) Eq. 5 reduces to Eq. 3. For deuterium-labeled ligands, rapid tumbling in both the free and bound states was assumed, resulting in complete averaging of quadrupolar splitting

interactions. When $\tau_e \ll \tau_M$ and $(\tau_e\omega)^2 \ll 1$, Eq. 5 reduces to:

$$J(\omega) = 2\left[\frac{S^2\tau_M}{1+\omega^2\tau_M^2} + (1-S^2)\tau_e\right] \quad (6)$$

Lipari and Szabo (1982a, b) have shown that if both conditions apply to the system under consideration, the internal motion information embedded in an NMR relaxation experiment is rigorously and completely specified by S^2 and τ_e. S^2 and τ_e may be obtained by performing T_1 or T_2 relaxation experiments in addition to the off-resonance rotating frame spin-lattice relaxation experiment, and the numerical values can be interpreted within the framework of a variety of models.

A simple model to enable a physical picture of the motion of μ is to assume diffusion within a cone of semiangle θ_o. For this model (Kinoshita et al., 1977; Howarth, 1979; Lipari and Szabo, 1980, 1981; Wang and Pecora, 1980),

$$S_{cone} = \frac{1}{2}(\cos\theta_o)(1+\cos\theta_o) \quad (7)$$

such that:

$$\theta_o = \cos^{-1}\left[\frac{1}{2}\{(1+8S_{cone})^{1/2} - 1\}\right] \quad (8)$$

if $0 \le \theta_o \le 90°$ is assumed. Thus, the motion of an attached deuterated ligand that is freely diffusing within the volume of a cone is described.

Theoretical simulations

A static field (B_o) of 7.05 T corresponding to the field strength used for the accompanying experiments was assumed in the theoretical simulations. In addition, a deuterium quadrupolar coupling constant (DQCC) of 170 kHz was employed for the simulations, which represents the average value for a deuterium nucleus attached to an sp^3 hybridized carbon (Mantsch et al., 1977). All simulations were carried out using programs written in Borland Turbo PASCAL (Ver. 5) and are available upon request by sending an E-mail request to yoti@aku.ucsc.edu.

Isotropic reorientation

Fig. 1 depicts computer simulations demonstrating the dependence of the ^{2}H spectral intensity ratio dispersion curves (R (= $\cos^2\Theta[T_{1\rho}^{off}/T_1]$) vs. ν_{off} at constant B_2 field strength) on the fraction of bound ligand (χ_B) (panel A), the isotropic rotational correlation times of the bound ($\tau_{o,B}$) (panel B), and the free ($\tau_{o,F}$) ligand species (panel C). Fast exchange between the free- and macromolecular-bound-ligand states was assumed. These simulations demonstrated the sensitivity of the intensity ratio dispersion curves to the fraction of bound ligand (panel A) at fraction bound values <0.14 ($\tau_{o,F}$ = 0.01 ns); whereas at fraction bound values >0.2, little or

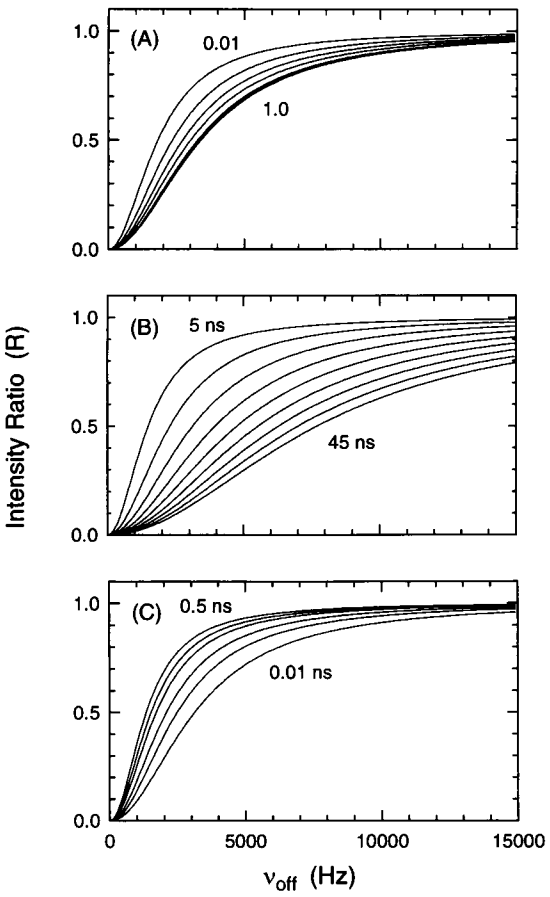

FIGURE 1 Simulated ^{2}H spectral intensity ratio dispersion curves (R (= $\cos^2\Theta[T_{1\rho}^{off}/T_1]$) vs. RF frequency offset, ν_{off}, at constant B_2 field strength) for different values of (A) fraction of bound ligand, χ_B; (B) rotational correlation time for bound ligand, $\tau_{o,B}$; (C) rotational correlation time of free ligand, $\tau_{o,F}$. Isotropic reorientational motion of the ligand in the free and bound states was assumed (see Theory section for additional details). Values for χ_B in panel (A) were: 0.01, 0.025, 0.05, 0.1, 0.3, 0.5, and 1.0; $\tau_{o,B}$ = 15 ns; $\tau_{o,F}$ = 0.01 ns. Values for $\tau_{o,B}$ in panel (B) were: 5, 10, 15, 20, 25, 30, 35, 40, and 45 ns; $\tau_{o,F}$ = 0.01 ns; χ_B = 0.14. Values for $\tau_{o,F}$ in panel (C) were: 0.5, 0.3, 0.2, 0.1, 0.05, and 0.01 ns; $\tau_{o,B}$ = 15 ns; χ_B = 0.14. For all simulations the following parameters were assumed: B_o = 7.05 T, DQCC = 170 kHz, off-resonance RF field strength (B_2) = 1.3 Gauss.

no change in dispersion curve behavior was observed. Fig. 1 also displays the sensitivity of the intensity ratio dispersion curves to changes in $\tau_{o,B}$ (panel B) and $\tau_{o,F}$ (panel C) at a fixed bound-ligand fraction value of 0.14 where the dispersion curves were found to be responsive to changes in these parameters.

Three-dimensional representations illustrating the dependence of the intensity ratio, R, on $\tau_{o,B}$ and χ_B at a ν_{off} value of 3500 Hz for different values of $\tau_{o,F}$ are shown in Fig. 2, A–C. For small values of χ_B at all values of $\tau_{o,F}$ considered, the off-resonance rotating frame spin-lattice relaxation experiment was observed to be highly sensitive to changes in χ_B, whereas with increased ligand binding, R leveled off to a value that reflected the motional parameters of the bound species. This effect was most apparent at both larger $\tau_{o,B}$ and smaller $\tau_{o,F}$ values. This observation suggested that in

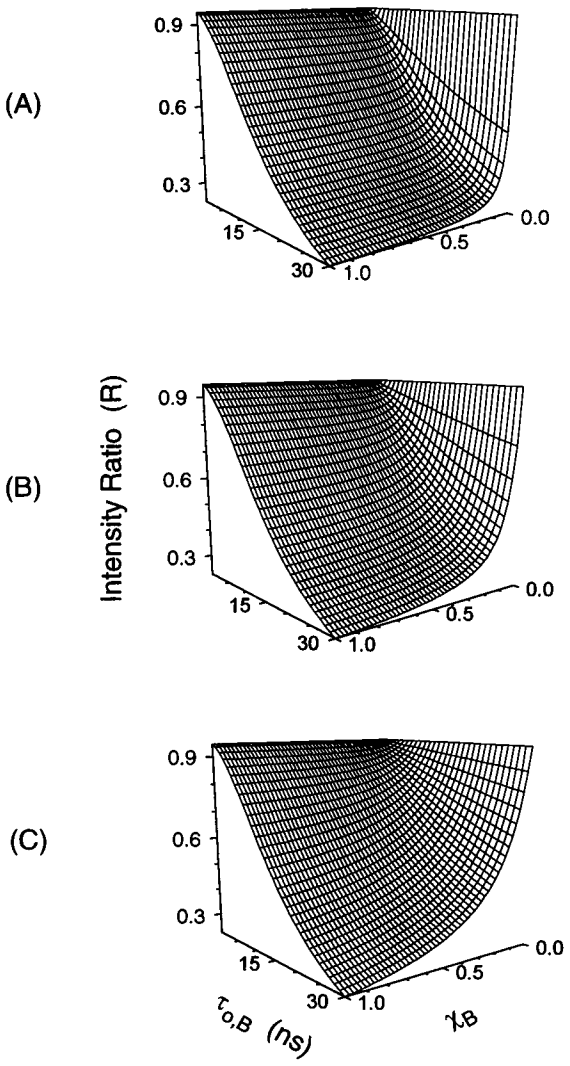

FIGURE 2 Simulated ^{2}H spectral intensity ratio (R (= $\cos^2\Theta[T_{1\rho}^{off}/T_1]$)) as a function of the fraction of bound ligand (χ_B) and the rotational correlation time of bound ligand ($\tau_{o,B}$) for different values of the rotational correlation of free ligand ($\tau_{o,F}$): (A) 0.01 ns, (B) 0.034 ns, and (C) 0.1 ns. Isotropic reorientational motion of the ligand in the free and bound states was assumed (see Theory section for additional details). For all simulations the following parameters were assumed: B_o = 7.05 T, DQCC = 170 kHz, off-resonance RF field strength (B_2) = 1.3 Gauss, frequency offset (ν_{off}) = 3500 Hz.

many cases involving the binding of a deuterated ligand to a macromolecular species, the intensity ratio primarily reflects the relaxation parameters characteristic of the bound species.

Bound ligand internal motion

The generalized order parameter (S^2) and the accompanying effective correlation time (τ_e) were incorporated into the ^{2}H off-resonance rotating frame spin-lattice relaxation experiment formalism to allow for the additional complexity of internal motion involving the ligand-bound state. In this case two unknown parameters occur, and thus a minimum of two relaxation measurements are necessary for quantitative evaluation of this experiment. Because of this, T_1 and T_2 relaxation behavior was also considered in addition to the off-resonance rotating frame spin-lattice relaxation experiment, thereby enabling selection of the appropriate [S^2, τ_e] pair from multiple pairs of [S^2, τ_e] solutions that would otherwise occur.

For the following computer simulations, fast exchange between free- and macromolecular-bound ligand was assumed. The free species was assumed to be tumbling isotropically, whereas the bound species was assumed to sustain internal motion superimposed on overall isotropic tumbling as described by Eq. 5. Figs. 3–6 depict sets of computer simulations demonstrating the dependence of T_1, T_2, and R on τ_e for different assumed values of τ_M, χ_B, τ_o,

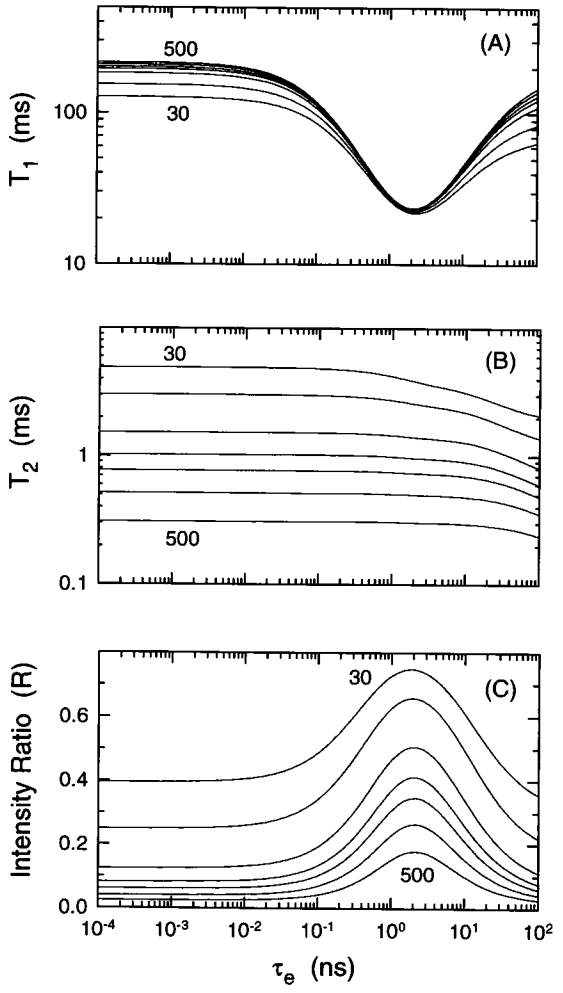

FIGURE 3 Simulated ^{2}H T_1 (A), T_2 (B), and spectral intensity ratio (R = $\cos^2\Theta[T_{1\rho}^{off}/T_1]$) ($C$) vs. effective correlation time (τ_e) curves for different values of the rotational correlation time of the macromolecule (τ_M). Isotropic reorientational motion was assumed for the free ligand, whereas internal motion was assumed for the bound ligand (see Theory section for additional details). For all simulations the following parameters were assumed: B_o = 7.05 T, S^2 = 0.36, χ_B = 0.14, $\tau_{o,F}$ = 0.012 ns, DQCC = 170 kHz. Values for τ_M were: 500, 300, 200, 150, 100, 50, and 30 ns. For (C) an off-resonance RF field strength (B_2) of 1.3 Gauss, and an RF frequency offset (ν_{off}) of 3500 Hz were assumed.

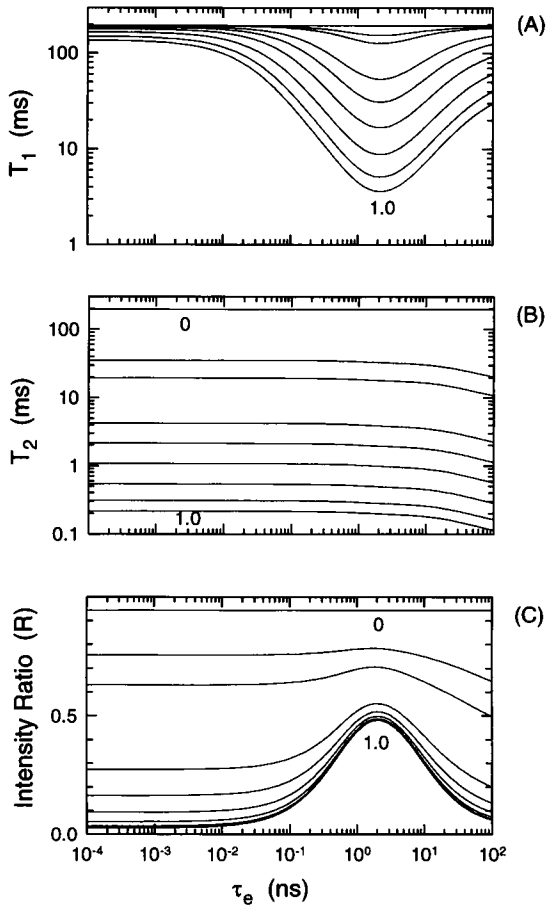

FIGURE 4 Simulated ^2H T_1 (A), T_2 (B), and spectral intensity ratio ($R = \cos^2\Theta[T_{1\rho}^{off}/T_1]$) ($C$) vs. effective correlation time (τ_e) curves for different values of the bound ligand fraction (χ_B). Isotropic reorientational motion was assumed for the free ligand, whereas internal motion was assumed for the bound ligand (see Theory section for additional details). For all simulation the following parameters were assumed: $B_o = 7.05$ T, $S^2 = 0.36$, $\tau_M = 100$ ns, $\tau_{o,F} = 0.012$ ns, and DQCC = 170 kHz. Values for χ_B were: 0, 0.005, 0.01, 0.05, 0.1, 0.2, 0.4, 0.7, and 1.0. For (C) an off-resonance RF field strength (B_2) of 1.3 Gauss, and an RF frequency offset (ν_{off}) of 3500 Hz were assumed.

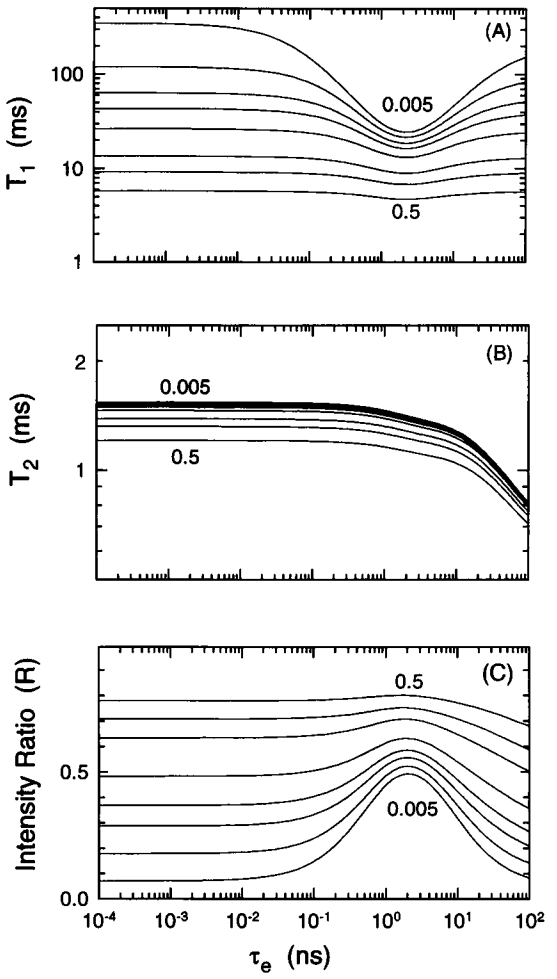

FIGURE 5 Simulated ^2H T_1 (A), T_2 (B), and spectral intensity ratio ($R = \cos^2\Theta[T_{1\rho}^{off}/T_1]$) ($C$) vs. effective correlation time (τ_e) curves for different values of the rotational correlation time of free ligand ($\tau_{o,F}$). Isotropic reorientational motion was assumed for the free ligand, whereas internal motion was assumed for the bound ligand (see Theory section for additional details). For all simulations the following parameters were assumed: $B_o = 7.05$ T, $S^2 = 0.36$, $\tau_M = 100$ ns, $\chi_B = 0.14$, and DQCC = 170 kHz. Values for $\tau_{o,F}$ were: 0.005, 0.02, 0.04, 0.06, 0.1, 0.2, 0.3, and 0.5 ns. For (C) an off-resonance RF field strength (B_2) of 1.3 Gauss, and an RF frequency offset (ν_{off}) of 3500 Hz were assumed.

and S^2. The parameters τ_M, χ_B, $\tau_{o,F}$, and S^2 were set equal to 100 ns, 0.14, 0.012 ns, and 0.36, respectively, when employed as fixed values in the simulations.

Little variation in T_1, T_2, or R as a function of τ_e was observed when τ_e was less than $\sim 10^{-2}$ ns, as a result of the dominance of the macromolecular tumbling contribution to the spectral density function (see Figs. 3–6). As τ_e increases, however, the internal motion begins to contribute significantly to the average T_1. Because R is a ratio involving T_1, this parameter increases accordingly. When $(\omega_o\tau_e)^2$ approaches 1, the spectral density function can no longer be adequately described by Eq. 6; and instead Eq. 5 applies, whereas when τ_e approaches τ_M, the internal motion becomes slow enough to reduce τ to a value that is in the slow motional regime, thereby increasing the average T_1. Because T_2 is dominated by $J(0)$, it is frequency independent up to very large values of τ_e.

Fig. 3 displays a set of computer simulations illustrating the dependence of the ^2H T_1 and T_2 relaxation times and the spectral intensity ratio (R (= $\cos^2\Theta[T_{1\rho}^{off}/T_1]$)) on τ_e given different values of τ_M. These simulations revealed that T_1 was the least sensitive parameter to differences in τ_M, whereas T_2 was found to be the most responsive. Because T_2 was found to be relatively constant over a broad range of τ_e values, it is an appropriate measurement to use for obtaining τ_M if all other parameters are known. Fig. 4 displays a set of computer simulations illustrating the dependence of T_1, T_2, and R on χ_B. This set of simulations revealed that T_1 was dependent on χ_B in the region of τ_e between 0.1 and 20 ns, but was not responsive to changes in bound-ligand fraction at τ_e values <0.01 ns. With the assumed values for S^2 and $\tau_{o,F}$, R and T_2 were observed to vary with χ_B, whereas R was

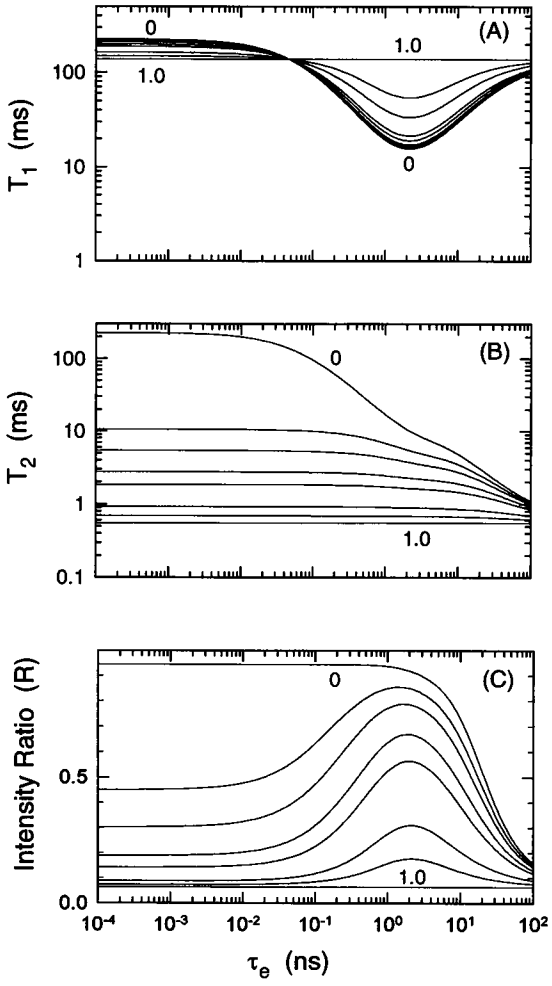

FIGURE 6 Simulated ^2H T_1 (*A*), T_2 (*B*), and spectral intensity ratio (R (= $\cos^2\Theta[T_{1\rho}^{off}/T_1]$)) (*C*) vs. effective correlation time (τ_e) curves for different values of the order parameter (S^2). Isotropic reorientational motion was assumed for the free species, whereas anisotropic tumbling was assumed for the bound species (see Theory section for additional details). For all simulations B_o = 7.05 T, $\tau_{o,F}$ = 0.012 ns, τ_M = 100 ns, χ_B = 0.14, and DQCC = 170 kHz. Values for S^2 were: 0.0, 0.05, 0.1, 0.2, 0.3, 0.6, 0.8, 1.0. For (*C*) an off-resonance RF field strength (B_2) of 1.3 Gauss, and an RF frequency offset (ν_{off}) of 3500 Hz were assumed.

more responsive at smaller bound fractions. Fig. 5 demonstrates the dependence of these parameters on τ_e at different values of $\tau_{o,F}$. These simulations revealed that T_2 was largely insensitive to the correlation time of the free species, whereas R and T_1 varied significantly with changes in $\tau_{o,F}$. Fig. 6 demonstrates the dependence of these parameters on the order parameter and furthermore, reveals that T_2 and R were more sensitive than T_1 to variations in S^2, particularly at small values of τ_e.

EXPERIMENTAL

NMR

^2H spectra and relaxation times were obtained at 46.07 MHz using a General Electric GN-300 spectrometer (currently serviced by Bruker, Billerica, MA) equipped with a Oxford Instruments (Oxford, UK) 7.05 T, wide bore (89 mm) magnet. A GE 12 mm broad-band probe and 12 mm (o.d.) NMR tubes (nonspinning) were used. T_1 and T_2 were measured using inversion recovery and the Hahn spin-echo experiment, respectively. Phase cycling was used for all measurements. ^2H chemical shifts were referenced to the natural abundance $^1H^2HO$ resonance at 4.76 ppm at 25°C. ^2H off-resonance rotating frame spin-lattice relaxation experiments using the NMR methodology previously described (Rydzewski and Schleich, 1994) were performed at 22°C on TSP-d_4-BSA solutions of known binding characteristics prepared by equilibrium dialysis (see below). This experiment was only conducted on those samples with ^2H resonance signals narrow enough to perform reasonable integrations. The spectral width used was ±2000 Hz and the B_2 power varied from 1.28 to 1.46 Gauss. ^2H T_1 and T_2 relaxation times for TSP-d_4 in the presence of BSA were also measured in selected samples.

Equilibrium dialysis binding measurements

BSA fraction V powder was purchased from Sigma (St. Louis, MO) and defatted essentially according to Chen (1967). The solution was passed through a 0.45-μ Millipore filter (Millipore Corp., Marlborough, MA) to ensure removal of residual charcoal. The polymer composition of the defatted BSA was determined by gel filtration HPLC using a BioSil Sec-250, 600 × 7.5-mm column (BioRad, Richmond, CA), with 150-mM NaCl in 5-mM phosphate buffer (pH 7.4) as the mobile phase. BSA concentrations were determined by UV absorbance at 280 nm using an extinction coefficient of $\epsilon_{280}^{0.1\%}$ = 0.62 (Rydzewski, 1992).

The experimentally determined oligomeric composition (by weight) of the defatted BSA used in these studies was 81.2% monomer, 14.9% dimer and ~3.0% trimer, 0.6% tetramer, and 0.3% pentamer.

The buffer used in the equilibrium dialysis experiment was 5-mM sodium phosphate containing 150-mM NaCl, pH 7.4. Dialysis tubing (Spectra/Por #2 tubing, molecular weight cut-off 12–14, PGC Scientifics, Gaithersburg, MD) was treated with EDTA and dithiothreitol at 90–100°C, followed by exhaustive washing with ultrapure water, before use. Defatted BSA was exhaustively dialyzed at 4°C against equilibrium dialysis buffer for use in binding experiments.

Sodium 3-(trimethylsilyl) propionate-2,2,3,3,-d_4 (TSP-d_4) (98 atom %) was purchased from Cambridge Isotopes (Woburn, MA). Both experimental and control samples were prepared for each TSP concentration used. The experimental sample for equilibrium dialysis was 3.5-mL BSA solution in buffer, at the appropriate concentration, which was placed into dialysis tubing, sealed, and inserted into a 20-mL screw-cap vial; a 3.5-mL aliquot of the appropriate TSP working solution was pipetted into the vial on the outside of the dialysis bag. A control sample was prepared in an identical manner, except that the protein solution was replaced by buffer inside the dialysis bag. As an experimental check, additional samples were prepared at a selected TSP concentration where the BSA concentration was about one-fourth of that of the other samples. The samples were allowed to equilibrate in the dialysis apparatus at 22°C for ~2 days with periodic agitation. To ensure that equilibrium had been reached, the inside and outside concentrations of TSP-d_4 in a control sample were checked to confirm that they were in fact equal. Binding measurements were based upon ^2H resonance intensity measurements of TSP made on aliquots removed from outside the dialysis bags.

Quantitation was performed by integration of the two TSP ^2H resonances in the NMR spectrum. The fraction of bound ligand was determined by the following relationship: $(I_{control} - I_{experimental})/I_{control}$, where $I_{experimental}$ and $I_{control}$ are the ^2H resonance intensities of the experimental and control samples representing total free ligand supporting equilibrium ligand binding and the total available ligand, respectively. The concentrations of TSP-d_4 present in the experimental and control solutions were determined by using the integrated areas of the TSP-d_4 NMR standard solutions as a reference. The relationship between the TSP-d_4 concentration and the ^2H resonance intensity was confirmed to be linear.

Data analysis

^{2}H off-resonance rotating frame spin-lattice relaxation experiment intensity ratio curves (R vs. ν_{off}) were analyzed as described previously (Rydzewski, 1992; Rydzewski and Schleich, 1994) using nonlinear regression to obtain values for the rotational correlation time and $R(\infty)$.

Equilibrium dialysis experimental data were analyzed using the Scatchard method. Equilibrium ligand-binding behavior is described by the following relationship, which assumes i classes of independent and equivalent macromolecular binding sites (Klotz, 1974; Cantor and Schimmel, 1980b; Zierler, 1989):

$$\frac{\bar{\upsilon}}{[L]_F} = \sum_{i=1}^{N}\left[\frac{n_i k_i}{1 + k_i[L]_F}\right] \tag{9}$$

where $\bar{\nu}$ is the average number of moles of ligand bound per mole of macromolecule, k_i is the intrinsic binding constant of ith class (M^{-1}), n_i is the number of binding sites of class i per mole of macromolecule, N is the total number of classes of binding sites, and $[L]_F$ is the concentration of the free ligand in equilibrium with the bound form. For a single class of equivalent and independent binding sites, a plot of $\bar{\nu}/[L]_F$ vs. $\bar{\nu}$ yields a straight line with a negative slope. For this case, the $\bar{\nu}/[L]_F$ intercept is $\Sigma n_i k_i$ and the $\bar{\nu}$ intercept is Σn_i (Klotz, 1974; Klotz and Hunston, 1979). By contrast, if the Scatchard plot is nonlinear, more than one class of binding sites are present, which may or may not display cooperative binding effects. A graphical procedure was used to extract the binding parameters (k_i and n_i) from the Scatchard plot following the procedure described by Cantor and Schimmel (1980b). To assess the validity of the binding parameters, the binding curve was reconstructed using Eq. 9 and the derived binding parameters.

RESULTS AND DISCUSSION

The goal of this study was to establish the feasibility and limitations of using the ^{2}H off-resonance rotating frame spin-lattice relaxation NMR experiment for the investigation of the rotational-diffusion behavior of ligands engaged in equilibrium binding to macromolecules. Consequently, NMR measurements were performed on samples of known binding characteristics prepared by equilibrium dialysis containing TSP-d_4 and BSA. The results of both equilibrium dialysis and companion magnetic resonance experiments are presented.

Experimental binding data for the binding of TSP-d_4 to BSA obtained from equilibrium dialysis experiments, and the subsequently derived parameters required for Scatchard plot analysis are tabulated in Table 1. The Scatchard plot corresponding to the data tabulated in Table 1 is shown in Fig. 7. The Scatchard plot is concave up implying the presence of more than one class of independent binding sites or the occurrence of anticooperative binding effects. Such behavior was expected, because it is known that BSA has at least two classes of binding sites, one of which binds ligands more tightly than the other (Klotz et al., 1948; Scatchard et al., 1957). The binding parameters obtained by Scatchard analysis were: $n_1 = 1$, $k_1 = 1600\ M^{-1}$; $n_2 = 11$, $k_2 = 50\ M^{-1}$. The relatively small values of the derived association constants indicate weak association between TSP-d_4 and BSA, in contrast to the behavior reported for many fatty acids, drugs, and dyes (Kragh-Hansen, 1981; Spector, 1975). The solid line shown in Fig. 7 represents the theoretical curve calculated using Eq. 9 and the derived binding parameter values with $N = 2$. This curve is in excellent agreement with the experimental data points thus supporting the validity of the derived binding parameters.

^{2}H off-resonance rotating frame spin-lattice relaxation experiments were performed on all protein samples containing TSP-d_4 except for the two with the lowest ligand-binding density. Representative ^{2}H spectra of TSP-d_4 in the presence of BSA, prepared by equilibrium dialysis to known binding characteristics, are shown in Fig. 8. Resonance 1 corresponds to the HDO resonance, whereas resonances 2 and 3 represent the two nonequivalent deuterium resonances for TSP-d_4. As shown by the spectra presented in Fig. 8 the TSP-d_4 resonances broaden and become less resolved, with increasing fraction of protein bound deuterated ligand.

For the analysis of the rotational-diffusion behavior of the TSP-d_4 ligand involved in equilibrium binding to BSA, three motional models were considered. The first model assumed fast exchange between free and bound states with

TABLE 1 Equilibrium dialysis ligand-binding data and parameters for the binding of TSP-d_4 to BSA (20°C, pH 7.4)

Sample no.	Fraction of bound ligand	[TSP] added (mM)	[BSA]* (mM)	[TSP]‡ free (mM)	[TSP]‡ bound (mM)	$\bar{\nu}$ (moles ligand/ mole protein)	$\bar{\nu}/[TSP]_F$ (M^{-1})
1	0.11 ± 0.01	4.92	0.22	4.22	0.50	2.27	539
2	0.14 ± 0.02	49.0	0.87	41.1	6.73	7.74	188
3	0.15 ± 0.01	49.2	0.81	41.8	7.20	8.89	213
4	0.15 ± 0.02	4.90	0.25	4.00	0.69	2.76	690
5	0.22 ± 0.02	19.7	0.75	14.2	4.01	5.35	377
6	0.27 ± 0.02	19.6	0.92	13.8	5.12	5.57	403
7	0.31 ± 0.03	9.80	0.88	6.56	2.96	3.36	513
8	0.32 ± 0.02	9.84	0.76	6.59	3.13	4.12	625
9	0.41 ± 0.02	4.90	0.87	2.78	1.92	2.21	794
10	0.43 ± 0.03	4.92	0.74	2.71	2.01	2.72	1002
11	0.50 ± 0.04	1.96	0.86	0.81	0.81	0.94	1163
12	0.63 ± 0.07	0.98	0.88	0.39	0.54	0.61	1573

*BSA molecular weight = 66.5 kDa.

‡Excludes TSP-d_4 bound to dialysis tubing and glass.

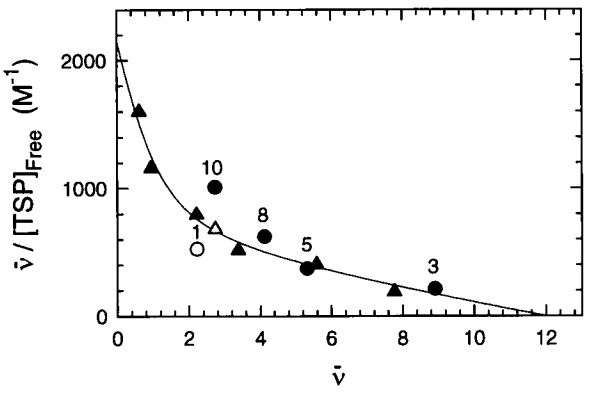

FIGURE 7 Scatchard plot for TSP-d_4 ligand binding to BSA. The calculated ligand binding parameters (see text for details) were: $n_1 = 1$, $k_1 = 1600\ M^{-1}$; $n_2 = 11$, $k_2 = 50\ M^{-1}$. The solid line is a simulated curve using Eq. 9 with $N = 2$. Off-resonance rotating frame spin-lattice relaxation experiments were performed on all protein samples with the exception of the two with the lowest binding density. The symbols ●, ▲ denote samples on which T_1 and T_2 measurements were also performed; open symbols signify samples containing 0.23–0.29 mM BSA, whereas filled symbols represent samples containing 0.75–0.90 mM BSA. A sample number accompanies selected symbols; see Table 1 for a tabulation of the relevant binding parameters.

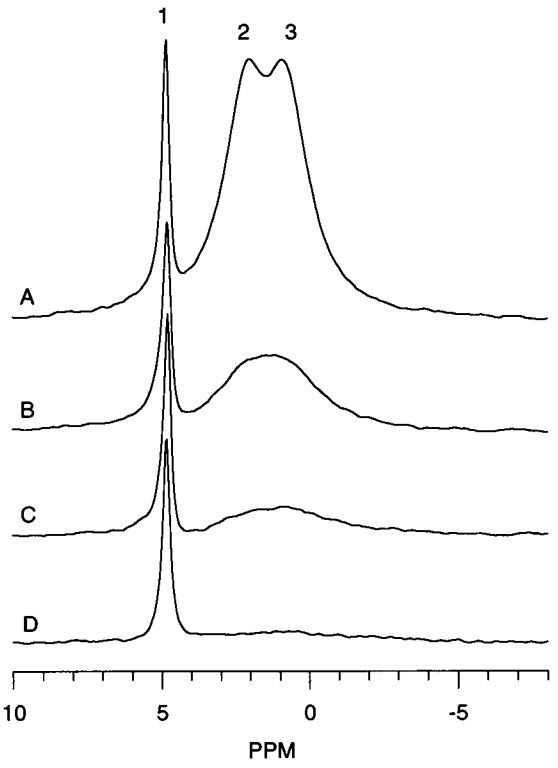

FIGURE 8 ^2H NMR spectra of TSP-d_4 in the presence of BSA at different values of the fraction of bound ligand. (*A*) $\chi_B = 0.15$ (sample 3); (*B*) $\chi_B = 0.22$ (sample 5); (*C*) $\chi_B = 0.32$ (sample 8); and (*D*) $\chi_B = 0.43$ (sample 10). Resonance 1 corresponds to the HDO resonance (4.76 ppm) whereas resonances 2 and 3 correspond to the two nonequivalent deuterium atoms of TSP-d_4. Each spectrum represents 64 acquisitions; 10-Hz line-broadening was applied to the free induction decay prior to Fourier transformation. See Table 1 for a tabulation of the relevant binding parameters.

both ligand states experiencing rigid rotor isotropic tumbling. The second model assumed a single molecular species tumbling isotropically with no distinction, and hence, no exchange, between free and bound states. This model, although unrealistic for the present study, was previously used for the investigation of rotational-diffusion characteristics of small molecules free in solution (Rydzewski and Schleich, 1994), and was nevertheless employed in the present study to enable assessment of the contribution that exchange between free and bound ligand states made to the derived rotational correlation time ($\tau_{o,eff}$). The third case considered was the same as the first, except that the bound-ligand species was assumed to be engaged in internal motion superimposed on overall macromolecular reorientational motion. The generalized order parameter approach of Lipari and Szabo (1982a, b) was used to characterize ligand motion occurring in the bound state. Implicit in these analyses was the assumption of identical ligand motional behavior characteristics for each of the two classes of binding sites on BSA.

Ligand isotropic rotational diffusion assuming fast exchange between free and bound ligand states and the absence of bound ligand internal motion

Representative experimental ^2H spectral intensity ratio dispersion curves (R (= M_z/M_o) vs. ν_{off} at constant B_2 field strength) for three representative samples, each reflecting different values of the fraction of bound ligand and ligand-binding density, prepared by BSA-TSP-d_4 equilibrium dialysis experiments are shown in Fig. 9, *A–C*. The solid line is the best fit curve obtained using an average value for the intensity of TSP-d_4 resonances 2 and 3, assuming fast exchange between bound and free species, and isotropic tumbling for ligand in both free and bound states. A correlation time for the free ligand of 0.012 ns that was obtained from a T_1 measurement of TSP-d_4 in buffer was used, assuming a DQCC of 170 kHz (Mantsch et al., 1977). These values were used as constants along with the relevant experimental fraction of bound ligand and B_2 RF field strength in the fitting routine; the correlation time for the bound species ($\tau_{o,B}$) and $R(\infty)$ were adjustable parameters. The theoretical fit was excellent for all experiments as shown in Fig. 9, *A–C*.

The experimental parameters and fitted $\tau_{o,B}$ values obtained for each TSP-d_4 resonance and for the combination of both resonance intensities are tabulated in Table 2. Both TSP-d_4 resonances behaved in approximately the same manner; the value of $\tau_{o,B}$ derived using resonance 2 was slightly larger than when resonance 3 was used in about half the samples. These small differences in rotational correlation time were attributed to experimental error, and we assumed that both resonances behaved in approximately the same manner. Thus, the reorientational motion of bound

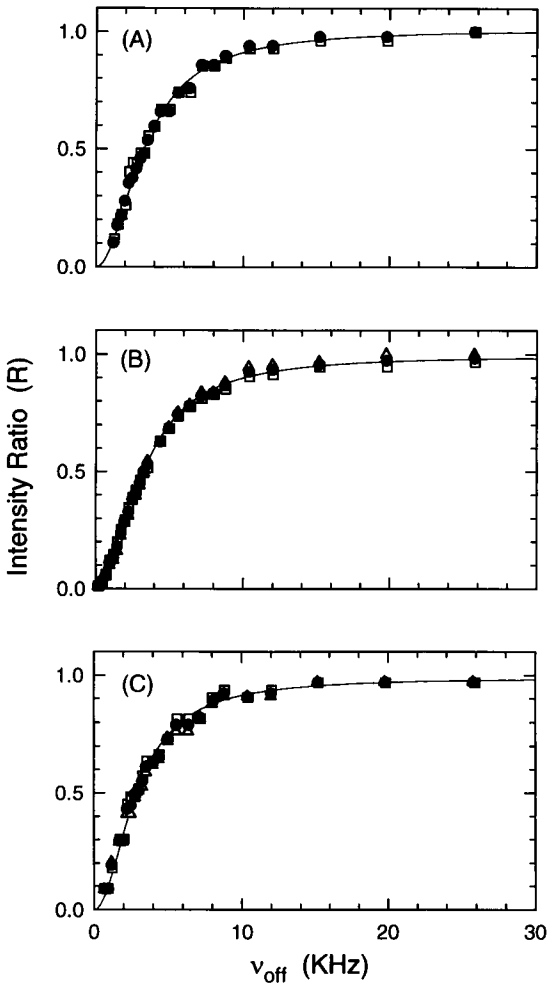

FIGURE 9 Experimental off-resonance rotating frame spin-lattice relaxation intensity ratio dispersion curves (R (= M_z/M_o) vs. RF frequency offset, ν_{off}, at constant B_2 field strength) for representative samples of TSP-d_4 in the presence of BSA prepared by equilibrium dialysis to different values of the fraction of bound ligand (χ_B). (A) χ_B = 0.43 (sample 10); (B) χ_B = 0.22 (sample 5); and (C) χ_B = 0.11 (sample 1). For all plots, (□) denotes the intensity ratio, R, derived from the TSP-d_4 resonance 2; whereas (△) denotes R derived from TSP-d_4 resonance 3; (●) denotes R derived from the combination of both resonances. The solid line is the best fit curve using the combination of resonances 2 and 3 assuming isotropic reorientation (see text for additional details). The following values were held constant in the fitting procedure: $\tau_{o,F}$ = 0.012 ns, DQCC = 170 kHz, whereas $\tau_{o,B}$ and $R(\infty)$ were adjustable parameters. Experimental binding parameters and the best fit values for $\tau_{o,B}$ and $\tau_{o,eff}$ are tabulated in Tables 1 and 2.

TSP-d_4, as reported by the deuterium nucleus, represents an overall molecular motion average rather than selective motion involving either the C2 or C3 positions of the ligand. In all cases the value for $\tau_{o,B}$ was approximately one-third the value of the calculated average rotational correlation time for BSA (see below), suggesting that a process faster than protein reorientational motion was contributing to the relaxation occurring in the bound state. Two appropriate candidates for this process are internal motion at the protein ligand-binding site(s) and/or contributions from chemical exchange.

Experimental magnetic relaxation parameters obtained as a function of bound-ligand fraction are tabulated in Table 3. Within experimental error, both resonances 2 and 3 of TSP-d_4 behaved in a similar fashion, with the possible exception of the T_1 relaxation time measurements for two samples (3 and 5), which were observed to be longer for TSP-d_4 resonance 2 than for resonance 3 by ~11%. However, in this study we assumed similar behavior for both resonances.

To examine the feasibility of assessing the fraction of bound deuterated ligand by analysis of intensity ratio dispersion curves (at least for small χ_B values) the following iterative procedure, in conjunction with the fast exchange isotropic tumbling model, was applied to data obtained using a sample of TSP-d_4 in the presence of BSA of known binding characteristics. For the given sample an experimental intensity ratio ($R = M_z/M_o$) value close to 0.5 and ^{2}H T_1 and T_2 relaxation time values were noted. The theoretical relaxation times T_1 and T_2, as well as the intensity ratio, R, were subsequently calculated using assumed pairs of [χ_B, $\tau_{o,B}$] values following procedures described in the Theory section, assuming a $\tau_{o,F}$ value of 0.012 ns and a DQCC of 170 kHz (Mantsch et al., 1977). The assumed fraction of bound ligand, χ_B, was varied from zero to one in small increments, and, in turn, at each incremental value of χ_B, $\tau_{o,B}$ was varied from 0.0001 to 1.83 ns in small steps. The value of $\tau_{o,B}$ at each increment of a given χ_B value was used to calculate a set of relaxation values. The value of $\tau_{o,B}$ that yielded a set of relaxation values closest to the corresponding experimental measurements (i.e., [T_1, T_2], [T_1, R], [T_2, R], or [T_1, T_2, R]) was used to calculate the absolute value of the sum of the relative differences between pairs of calculated and experimental values; this value, which is a reflection of the error was denoted by Δ. This calculation was also repeated in the same manner except that the range of assumed $\tau_{o,B}$ values was varied from 2 to 100 ns. This second calculation was necessary because of the parabolic dependence of T_1 on $\tau_{o,B}$, which has a minimum at ~2 ns as shown in Fig. 3 A. Examples of the results of these calculations, which are shown in Figs. 10 and 11, assumed $\tau_{o,B}$ values from 0.0001 to 1.83 ns and 2 to 100 ns, respectively, for sample 5. The solid line is Δ, whereas the dotted line is the $\tau_{o,B}$ value at a particular incremental value of χ_B. The vertical arrow denotes the value of the experimental fraction of bound ligand obtained from equilibrium dialysis binding experiments. Plots associated with the four other BSA samples in which T_1 and T_2 measurements were made were all found to be similar (not shown). The value of Δ was relatively large and failed to reach a minimum using any combination of relaxation measurements when short $\tau_{o,B}$ times were employed; by contrast, a minimum in Δ was obtained when longer $\tau_{o,B}$ values were used, as shown in Fig. 11. For each sample, the minimum in Δ occurred at approximately the same χ_B value for any combination of relaxation measurements, but was smaller than the experimental value for all protein samples studied. These results indicated that the use of any combination of relaxation

TABLE 2 Values of the effective ($\tau_{o,eff}$) and bound ($\tau_{o,B}$) ligand rotational correlation times as a function of bound ligand fraction (χ_B) for the binding of TSP-d_4 to BSA (22°C, pH 7.4)

Sample no.	Bound ligand fraction (χ_B)	B_2 power (Gauss)	$\tau_{o,eff}$ (ns)			$\tau_{o,B}$ (ns)			δ* (ns)
			TSP-d_4 resonance 2	TSP-d_4 resonance 3	TSP-d_4 resonances 2 and 3 combined	TSP-d_4 resonance 2	TSP-d_4 resonance 3	TSP-d_4 resonances 2 and 3 combined	
1	0.11 ± 0.01	1.46	10.7 ± 0.3	10.6 ± 0.3	10.7 ± 0.3	12.2 ± 0.3	12.1 ± 0.5	12.2 ± 0.4	1.5
2	0.14 ± 0.02	1.33	11.1 ± 0.2	11.5 ± 0.2	11.2 ± 0.2	12.7 ± 0.3	12.2 ± 0.2	12.4 ± 0.2	1.2
3	0.15 ± 0.01	1.40	13.3 ± 0.2	11.7 ± 0.2	12.4 ± 0.2	14.8 ± 0.3	12.9 ± 0.2	13.8 ± 0.2	1.4
4	0.15 ± 0.02	1.30	11.2 ± 0.4	10.6 ± 0.3	11.1 ± 0.2	12.3 ± 0.4	11.6 ± 0.4	12.2 ± 0.3	1.1
5	0.22 ± 0.02	1.46	12.8 ± 0.2	12.1 ± 0.2	12.5 ± 0.2	13.7 ± 0.2	12.9 ± 0.2	13.3 ± 0.2	0.8
6	0.27 ± 0.02	1.30	14.1 ± 0.3	12.6 ± 0.2	13.3 ± 0.2	14.8 ± 0.3	13.3 ± 0.2	14.0 ± 0.2	0.7
7	0.31 ± 0.03	1.32	12.6 ± 0.5	13.2 ± 0.5	12.8 ± 0.3	12.9 ± 0.6	13.7 ± 0.5	13.3 ± 0.4	0.5
8	0.32 ± 0.02	1.44	13.0 ± 0.4	12.0 ± 0.2	12.5 ± 0.2	13.7 ± 0.4	12.4 ± 0.2	13.0 ± 0.2	0.5
9	0.41 ± 0.02	1.28	10.2 ± 0.5	12.6 ± 0.8	10.0 ± 0.4	10.4 ± 0.5	13.0 ± 0.8	10.2 ± 0.2	0.2
10	0.43 ± 0.03	1.42	13.8 ± 0.3	12.7 ± 0.3	13.2 ± 0.2	14.1 ± 0.3	13.0 ± 0.4	13.5 ± 0.3	0.3

*$\delta = (\tau_{o,B} - \tau_{o,eff})$.

TABLE 3 ^{2}H T_1 and T_2 relaxation times as a function of bound ligand fraction (χ_B) for the binding of TSP-d_4 to BSA (22°C, pH 7.4)

Sample no.	Bound ligand fraction (χ_B)	T_1 (ms)			T_2 (ms)		
		TSP-d_4 resonance 2	TSP-d_4 resonance 3	TSP-d_4 resonances 2 and 3 combined	TSP-d_4 resonance 2	TSP-d_4 resonance 3	TSP-d_4 resonances 2 and 3 combined
3	0.15 ± 0.01	59.4 ± 0.5	53.6 ± 0.6	56.6 ± 0.2	4.30 ± 0.06	4.40 ± 0.08	4.35 ± 0.06
5	0.22 ± 0.02	41.7 ± 0.6	37.3 ± 0.4	39.5 ± 0.4	2.77 ± 0.05	2.71 ± 0.03	2.73 ± 0.03
8	0.32 ± 0.02	28 ± 1	30.7 ± 0.9	29.7 ± 1	2.12 ± 0.09	2.15 ± 0.08	2.11 ± 0.05
10	0.43 ± 0.3	30 ± 1	28 ± 1	28.8 ± 1	1.47 ± 0.08	1.48 ± 0.07	1.47 ± 0.07

measurements resulted in an underestimation of the experimental value of χ_B for sample 5 by 14–32% presumably as a consequence of internal motion of the bound ligand (see below). Furthermore, measurements incorporating T_1 relaxation times appeared to be the most sensitive to changes in χ_B, whereas T_2 and R measurements showed somewhat less sensitivity to changes in this binding parameter. The calculated values of $\tau_{o,B}$ at the minimum in Δ were in good agreement (within 14% for sample 5) with those derived by using nonlinear regression of the entire intensity ratio dispersion curve and the experimental value of χ_B.

Ligand isotropic rotational diffusion assuming the absence of exchange between free and ligand bound states

The values for $\tau_{o,eff}$ obtained using nonlinear regression, assuming a single ligand species tumbling isotropically, derived from ^{2}H off-resonance rotating frame spin-lattice relaxation intensity ratio dispersion curves are tabulated in Table 2. Analysis using resonance 2 of TSP-d_4 appeared to yield a slightly longer value for $\tau_{o,eff}$ than for resonance 3 for approximately half the samples studied, a characteristic noted in the analysis described above assuming fast exchange. This difference was attributed to experimental error and therefore neglected. The theoretical fits were excellent in all cases. All fitted $R(\infty)$ values were within 5% of the limiting value of 1.00. The best fit curves were superimposable (data not shown) with those presented for the fast exchange case discussed above. This finding implies that the off-resonance rotating frame spin-lattice relaxation formalism is applicable to both cases, and furthermore that a specific model of binding should be assumed before the assessment of motional parameters.

Because the observed rotational correlation time reflects a complicated average of molecular motions, including the effects of anisotropic motion, τ_o in reality is an effective correlation time, $\tau_{o,eff}$. The magnitude of the rotational correlation time, $\tau_{o,eff}$, particularly at larger values of the fraction of bound ligand, was attributed to be primarily a reflection of molecular motion associated with the bound fraction, a reasonable conclusion given that free TSP-d_4 yields essentially no intensity ratio dispersion curve (data not shown). In addition, comparison of the rotational correlation time values in Table 2 obtained by assuming a nonexchange condition with that obtained by assuming a fast exchange model, revealed that at bound fractions at or greater than ~0.15, there was less than a 12% difference between $\tau_{o,eff}$ and $\tau_{o,B}$, which decreased to smaller values with increasing values of bound-ligand fraction (see Table 2). This observation supports the point made above that the motional dynamics of the bound species can be extracted directly from the off-resonance rotating frame spin-lattice relaxation experiment when the fraction of bound ligand is larger than some minimal value, in this case 0.15, without assuming a value for DQCC or invoking a motional model.

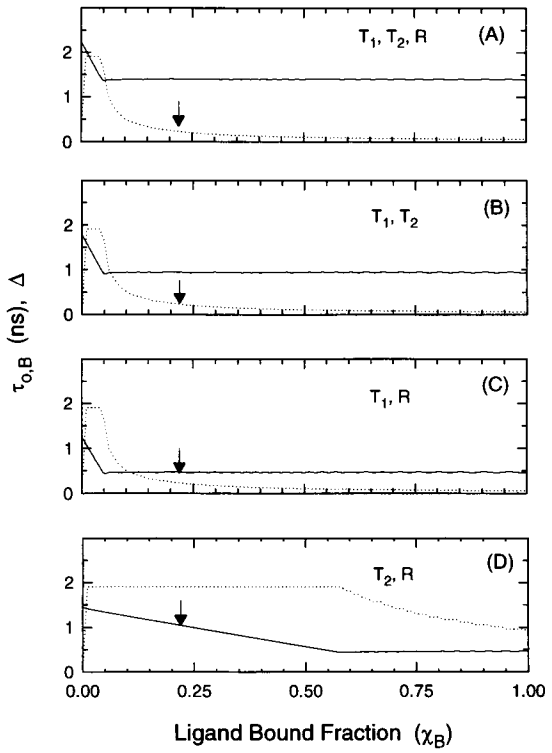

FIGURE 10 Representative plots displaying the iterated assumed values of the rotational correlation time of bound ligand ($\tau_{o,B}$) and the absolute value of the sum of the relative difference between pairs of theoretically calculated and experimental relaxation parameters (Δ) vs. the iterated fraction of bound TSP-d_4 (χ_B) for sample 5. The assumed $\tau_{o,B}$ values varied from 0.0001 to 1.83 ns in small increments. The solid line represents Δ, whereas the dotted line describes the trajectory that the assumed value of $\tau_{o,B}$ makes in respect to χ_B. The sets of experimental measurements considered were: (*A*) T_1, T_2, R; (*B*) T_1, T_2; (*C*) T_1, R; (*D*) T_2, R. The vertical arrows denote the value of the experimental fraction of bound ligand obtained from equilibrium dialysis measurements. Isotropic tumbling of the ligand in the free and bound states and fast exchange were assumed. See text for additional details.

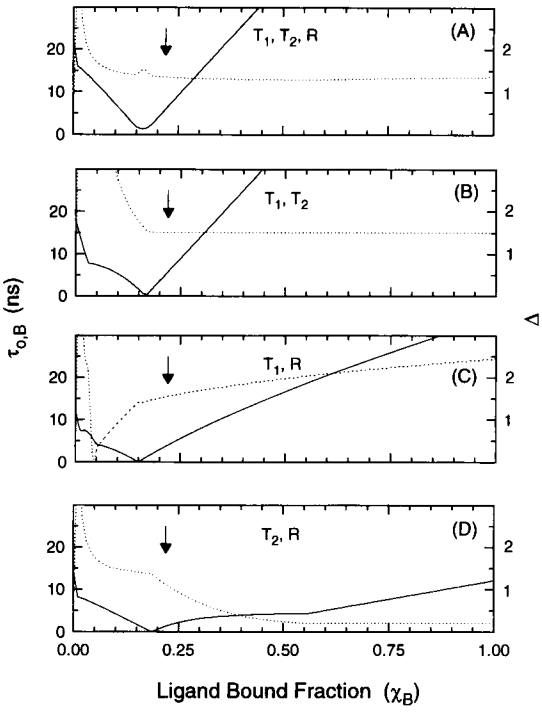

FIGURE 11 Representative plots displaying the iterated assumed values of the rotational correlation time of bound ligand ($\tau_{o,B}$) and the absolute value of the sum of the relative difference between pairs of theoretically calculated and experimental relaxation parameters (Δ) vs. the iterated fraction of bound TSP-d_4 (χ_B) for sample 5. The assumed $\tau_{o,B}$ values varied from 2 to 100 ns in small increments. The solid line represents Δ, whereas the dotted line is the trajectory of the assumed value of $\tau_{o,B}$ makes in respect to χ_B. The sets of experimental measurements considered were: (*A*) T_1, T_2, R; (*B*) T_1, T_2; (*C*) T_1, R; (*D*) T_2, R. The vertical arrows denote the value of the experimental fraction of bound ligand obtained from equilibrium dialysis measurements. Isotropic tumbling of the ligand in the free and bound states and fast exchange were assumed. See text for additional details.

Ligand isotropic rotational diffusion assuming the presence of fast exchange between free and bound ligand states and the presence of bound ligand internal motion

The third model assumed isotropic tumbling of the free ligand species and internal or local motion of the bound ligand, superimposed on overall isotropic reorientational motion of the macromolecule. Contributions to relaxation from chemical exchange effects were ignored. The generalized order parameter approach of Lipari and Szabo (1982a, b) was used to describe the ligand motional behavior in this case. The apparent relaxation rates were calculated as described in the Theory section using spectral density functions defined by Eq. 3 (isotropic tumbling), and Eqs. 4 or 5 (anisotropic tumbling due to bound ligand internal motion). For this analysis, both the rotational correlation times of the free ligand and the macromolecule, τ_M, were required. A value of 37 ns was calculated for the average isotropic correlation time of the oligomeric BSA preparation, free in solution (corrected for finite protein concentration (Koenig, 1980; Schleich et al., 1992)), from the weight composition using the following macromolecular parameters: partial specific volume = 0.734 cm^3/g, molecular mass = 66.5 kDa, hydration = 0.4 g water/g protein (Cantor and Schimmel, 1980a), and temperature = 295 K. The experimental value of the rotational correlation time ($\tau_{o,eff}$) for unfractionated BSA determined by ^{13}C off-resonance rotating frame spin-lattice relaxation measurements was 50 ns; correction for anisotropic reorientational motion and finite protein concentration yielded a value of 28 ns (Wang et al., 1993). The calculated average value of the rotational correlation time employed in these studies is within these experimental values.

Calculations of the order parameter (S) and the effective correlation time (τ_e) were performed in a manner analogous to the isotropic fast exchange case considered above on data obtained from sample of TSP-d_4 in the presence of BSA. At each assumed χ_B value, S^2 was varied from 0 to 1, whereas τ_e was varied from 0.0001 to 1.83 ns at each S^2 value in small increments. Theoretical T_1, T_2, and R values were

calculated using each [S^2, τ_e] pair at a given assumed χ_B value, and the result compared with the experimental measurements for the given sample. The values of S^2 and τ_e yielding calculated relaxation values closest to combinations of experimental measurements were used. The calculation was also repeated by varying τ_e in the range 1.8 to 100 ns. Two ranges of τ_e were considered because of the parabolic behavior of T_1 and R on τ_e as shown by the simulations in Figs. 3–6.

Values for τ_e, S^2, and θ_o were calculated for samples 3, 5, 8, and 10, which contained approximately the same concentration of BSA; the fraction of bound ligand and NMR experimental parameters characterizing these samples are summarized in Table 4. Each of these samples, prepared by equilibrium dialysis, represented a different known amount of the fraction of bound ligand (TSP-d_4), to BSA (see Table 1). The values derived for both τ_e and S^2 are tabulated in Tables 5 and 6. All the values for τ_e were found to be in the range of 0.20 to 0.36 ns regardless of the relaxation parameters employed in the calculation. Likewise, the calculated S^2 values range from 0.20 to 0.33. These results indicated that the motional time scale of the bound ligand (τ_e) was at least 100 times smaller than the correlation time characterizing overall tumbling of the macromolecule (τ_M). Because the conditions $\tau_M \gg \tau_e$ and $\omega^2\tau_e^2 \ll 1$ were fulfilled for the binding of TSP-d_4 to BSA, the wobbling in the cone model was applicable to the motion of μ and was used to describe a physical picture for the motion of ligand in the bound state; θ_o values were calculated using Eq. 8. These values are tabulated in Table 7 and were found to be in the range of 45 to 56°. This indicates a wide range of allowed motion for the bound ligand suggesting a weak interaction at the binding site, and it is consistent with the small binding constants obtained for the binding of TSP-d_4 to BSA.

When all assumed values of χ_B were considered in addition to the experimental values of χ_B, an infinite number of combinations of τ_e, S^2, and χ_B above a certain minimum value of χ_B were found to satisfy the experimental relaxation parameters in all cases considered. Thus, if the fraction of bound ligand is not known from independent binding measurements, only a range for S^2 and τ_e can be ascertained.

TABLE 4 Experimental parameters used for the calculation of the order parameter (S^2) and effective correlation time (τ_e) as a function of bound ligand fraction (χ_B) for the binding of TSP-d_4 to BSA (22°C, pH 7.4)*

Sample no.	Bound ligand fraction (χ_B)	B_2 power (Gauss)	ν_{off} (Hz)	R
3	0.15 ± 0.01	1.40	3284.5	0.5085
5	0.22 ± 0.02	1.46	3280.8	0.4994
8	0.32 ± 0.02	1.44	3283.0	0.4902
10	0.43 ± 0.03	1.42	3536.0	0.5365

*τ_M = 37 ns, $\tau_{o,F}$ = 0.012 ns, DQCC = 170 kHz.

TABLE 5 Calculated values for the effective rotational correlation time (τ_e) obtained for TSP-d_4 binding to BSA (22°C, pH 7.4) employing various experimental ^{2}H relaxation parameters for samples of different ligand bound fraction (χ_B)*

Sample no.	τ_e using T_1, T_2 (ns)	τ_e using T_1, R (ns)	τ_e using T_2, R (ns)	τ_e using T_1, T_2, R (ns)	Δ‡
3	0.25 ± 0.02	0.25 ± 0.03	0.27 ± 0.03	0.25 ± 0.03	0.022
5	0.28 ± 0.05	0.27 ± 0.04	0.38 ± 0.06	0.28 ± 0.05	0.111
8	0.26 ± 0.02	0.26 ± 0.02	0.30 ± 0.03	0.26 ± 0.03	0.057
10	0.20 ± 0.02	0.19 ± 0.02	0.36 ± 0.04	0.20 ± 0.02	0.259

*See Table 4.
‡Δ is the sum of the absolute value of the minimum relative errors between the calculated and experimental measurements used in calculating [τ_e, S^2] pairs using all three relaxation measurements.

TABLE 6 Calculated values for the order parameter (S^2) obtained for the binding of TSP-d_4 to BSA (22°C, pH 7.4) employing various experimental ^{2}H relaxation parameters for samples of different ligand bound fraction (χ_B)*

Sample no.	S^2 (using T_1, T_2)	S^2 (using T_1, R)	S^2 (using T_2, R)	S^2 (using T_1, T_2, R)
3	0.30 ± 0.02	0.29 ± 0.02	0.30 ± 0.02	0.30 ± 0.02
5	0.33 ± 0.03	0.26 ± 0.03	0.32 ± 0.03	0.33 ± 0.03
8	0.29 ± 0.02	0.26 ± 0.02	0.28 ± 0.02	0.29 ± 0.02
10	0.32 ± 0.02	0.20 ± 0.02	0.31 ± 0.02	0.32 ± 0.02

*See Table 4.

TABLE 7 Calculated values of the cone semiangle (θ_o)* obtained for bound TSP-d_4 binding to BSA employing various experimental ^{2}H relaxation parameters for samples of different ligand bound fraction (χ_B)‡

Sample no.	θ_o (using T_1, T_2)	θ_o (using T_1, R)	θ_o (using T_2, R)	θ_o (using T_1, T_2, R)
3	49°	49°	49°	49°
5	47°	51°	48°	47°
8	50°	52°	50°	50°
10	48°	56°	48°	48°

*Assuming a wobbling in the cone model, see text for details.
‡See Table 4.

SUMMARY

The results of this study demonstrate that for deuterated ligands engaged in equilibrium binding to macromolecules, the motional behavior of the bound ligand species can be monitored directly by use of the ^{2}H off-resonance rotating frame spin-lattice relaxation experiment, which is applicable to both in vitro and in vivo situations. This was shown by the finding that the observed correlation time of the TSP-d_4 ligand in the presence of BSA was approximately equal to the rotational correlation time in the bound state, provided that the fraction of bound ligand was at least 0.20. This property of the ^{2}H off-resonance experiment is highly advantageous in systems where only the magnitude of the bound fraction is known. The assessment of the observed rotational correlation time ($\tau_{o,eff}$) was accomplished without the assumption of a value for the deuterium quadrupolar coupling constant or by invoking a particular motional model. The rotational correlational time of the bound ligand

was determined by assuming a two-state fast exchange isotropic tumbling model. The presence of internal or local ligand motion in the bound state, relative to the overall tumbling of the macromolecule and/or the occurrence of chemical exchange contributions, was implied by the observation that the rotational correlation time for bound ligand was somewhat smaller than the value for the rotational correlation time of the protein. Because the details of bound ligand motion are unknown it was not possible to distinguish between the two contributions. Furthermore, an approximate value (±32%) for the fraction of bound ligand could be determined if a supplemental T_1 and/or T_2 relaxation time was included in the analysis that assumed a two-state fast exchange isotropic tumbling motion model.

Incorporation of internal motion effects for the bound species into the theoretical relaxation formalism of the off-resonance rotating frame spin-lattice relaxation experiment, coupled with supplemental relaxation measurements (T_1 or T_2), yielded an order parameter and effective correlation time whose values, in conjunction with the assumption of a wobbling in the cone model, defined a cone of semiangle θ_o, thereby providing insights into the motional details of the bound ligand. Whereas TSP-BSA binding represents one model example, the ^{2}H off-resonance experiment can be used to provide relative motional time scales for a series of deuterated bound ligands. Although auxiliary measurements on other nuclei of the bound ligand, e.g., ^{13}C, or the use of other relaxation experiments could provide additional parameters to describe specific local fluctuations, the ^{2}H off-resonance rotating frame experiment supplemented with ^{2}H T_1 or T_2 measurements is useful for the determination of the relative binding characteristics of a suite of deuterated ligands without resorting to further isotopic labeling.

This research was supported by National Institutes of Health Grant EY 04033. We thank Mr. James Loo for providing outstanding technical support.

REFERENCES

Cantor, C. R., and P. R. Schimmel. 1980a. Biophysical Chemistry Part II: Techniques for the Study of Biological Structure and Function, W. H. Freeman and Co., San Francisco. 552.

Cantor, C. R., and P. R. Schimmel. 1980b. Biophysical Chemistry Part III: Behavior of Biological Macromolecules, W. H. Freeman and Co., San Francisco, 858–859.

Chen, R. F. 1967. Removal of fatty acids from serum albumin by charcoal treatment. *J. Biol. Chem.* 242:173–181.

Howarth, O. W. 1979. Effect of internal librational motions on the ^{13}C nuclear magnetic resonance relaxation time of polymers and peptides. *J. Chem. Soc. Faraday Trans. II.* 75:863–873.

Kinoshita, K., Jr., S. Kawato, and A. Ikegami. 1977. A theory of fluorescence polarization decay in membranes. *Biophys. J.* 20:289–305.

Klotz, I. M. 1974. Protein interactions with small molecules. *Accounts. Chem. Res.* 7:162–168.

Klotz, I. M., and D. L. Hunston. 1979. Protein affinities for small molecules: conceptions and misconceptions. *Arch. Biochem. Biophys.* 193:314–328.

Klotz, I. M., H. Triwush, and F. M. Walker. 1948. The binding of organic ions by proteins. Competition phenomena and denaturation effects. *J. Am. Chem. Soc.* 70:2935–2941.

Koenig, S. H. 1980. The dynamics of water-protein interactions. Results from measurements of nuclear magnetic relaxation dispersion. *In* American Chemical Society Symposium Series Water in Polymers. S. P. Rowland, editor. American Chemical Society, Washington, DC. 127: 157–176.

Kragh-Hansen, U. 1981. Molecular aspects of ligand binding to serum albumin. *Pharmacol. Rev.* 33:17–53.

Lipari, G., and A. Szabo. 1980. Effect of librational motion on fluorescence depolarization and nuclear magnetic resonance relaxation in macromolecules and membranes. *Biophys. J.* 30:489–506.

Lipari, G., and A. Szabo. 1981. Pade approximants to correlation functions for restricted rotational diffusion. *J. Chem. Phys.* 75:2971–2976.

Lipari, G., and A. Szabo. 1982a. Model-free approach to the interpretation of nuclear magnetic resonance relaxation in macromolecules. 1. Theory and range of validity. *J. Am. Chem. Soc.* 104:4546–4559.

Lipari, G., and A. Szabo. 1982b. Model-free approach to the interpretation of nuclear magnetic resonance relaxation in macromolecules. 2. Analysis of experimental results. *J. Am. Chem. Soc.* 104:4559–4570.

Mantsch, H. H., H. Saito, and C. P. Smith. 1977. Deuterium magnetic resonance, applications in chemistry, physics and biology. *Prog. NMR Spectroscopy.* 11:211–272.

Marshall, A. G. 1970. Calculation of NMR relaxation times for quadrupolar nuclei in the presence of chemical exchange. *J. Chem. Phys.* 52: 2527–2534.

Rose, K., and R. G. Bryant. 1978. Electrolyte ion correlation times at protein binding sites. *J. Magn. Reson.* 31:41–47.

Rydzewski, J. M. 1992. Application of ^{2}H and ^{13}C nuclear magnetic resonance spectroscopy to model and tissue systems. Ph.D. thesis. University of California, Santa Cruz. 363 pages.

Rydzewski, J. M., and T. Schleich. 1994. Off-Resonance rotating frame spin-lattice relaxation of quadrupolar (spin 1) nuclei. *J. Magn. Reson.*, Series B 105:129–136.

Scatchard, G., J. S. Coleman, and A. L. Shen. 1957. Physical chemistry of protein solutions. VII. The binding of some small anions to serum albumin. *J. Am. Chem. Soc.* 79:12–20.

Schleich, T., G. H. Caines, and J. M. Rydzewski. 1992. Off-Resonance rotating frame spin-lattice relaxation: Theory, and in vivo MRS and MRI applications. *In* Biological Magnetic Resonance. L. Berliner, and J. Reuben, editors. Plenum Press, New York. 11:55–134.

Schleich, T., C. F. Morgan, and G. H. Caines. 1989. Determination of protein rotational correlation times by carbon-13 rotating frame spin lattice relaxation in the presence of an off-resonance radiofrequency field. *Methods Enzymol.* 176:386–418.

Spector, A. 1975. Fatty acid binding to plasma albumin. *J. Lipid Res.* 16:165–179.

Wang, C. C., and R. Pecora. 1980. Time-correlation functions for restricted rotational diffusion. *J. Chem. Phys.* 72:5333–5340.

Wang, S. X., A. Stevens, and T. Schleich. 1993. Assessment of protein rotational diffusion by ^{13}C off-resonance rotating frame spin-lattice relaxation: Effect of backbone and side-chain internal motion. *Biopolymers.* 33:1581–1589.

Zierler, K. 1989. Misuse of nonlinear Scatchard plots. *TIBS* 14:314–317.